ACS Chemical Neuroscience

pubs.acs.org/chemneuro

Research Article

Dissecting the Structural Organization of Multiprotein Amyloid Aggregates Using a Bottom-Up Approach

Himanshu Chaudhary, Sebastian W. Meister, Henrik Zetterberg, John Löfblom, and Christofer Lendel*

Cite This: https://dx.doi.org/10.1021/acschemneuro.0c00110

Read Online

ACCESS | Metrics & More | Article Recommendations | Supporting Information

ABSTRACT: Deposition of fibrillar amyloid β (Aβ) in senile plaques is a pathological signature of Alzheimer's disease. However, senile plaques also contain many other components, including a range of different proteins. Although the composition of the plaques can be analyzed in post-mortem tissue, knowledge of the molecular details of these multiprotein inclusions and their assembly processes is limited, which impedes the progress in deciphering the biochemical mechanisms associated with Aβ pathology. We describe here a bottom-up approach to monitor how proteins from human cerebrospinal fluid associate with Aβ amyloid fibrils to form plaque particles. The method combines flow cytometry and mass spectrometry proteomics and allowed us to identify and quantify 128 components of the captured multiprotein aggregates. The results provide insights into the functional characteristics of the sequestered proteins and reveal distinct interactome responses for the two investigated Aβ variants, Aβ(1−40) and Aβ(1−42). Furthermore, the quantitative data is used to build models of the structural organization of the multiprotein aggregates, which suggests that Aβ is not the primary binding target for all the proteins; secondary interactions account for the majority of the assembled components. The study elucidates how different proteins are recruited into senile plaques and establishes a new model system for exploring the pathological mechanisms of Alzheimer's disease from a molecular perspective.

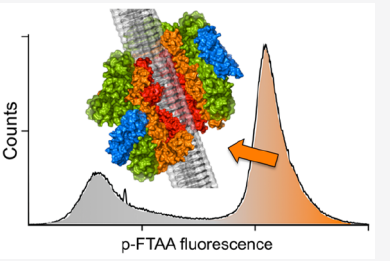

KEYWORDS: *amyloid, Alzheimer's disease, amyloid β, protein−protein interaction, flow cytometry*

INTRODUCTION

Neurodegenerative disorders are among the major medical challenges for the future. A pathological signature that is shared by several of these conditions (including, e.g., Alzheimer's and Parkinson's diseases) is the accumulation of certain proteins in amyloid structures in the central nervous system.[1] Alzheimer's disease (AD) is associated with two types of protein inclusions: intracellular neurofibrillary tangles made mainly from hyperphosphorylated protein tau and extracellular senile plaques with amyloid β (Aβ) as key building block.[2] Accumulation of Aβ in cerebral vasculature leading to cerebral amyloid angiopathy is also observed in the majority of AD cases.[3] Notably, senile plaques, as well as neurofibrillary tangles and most other pathological protein inclusions, do not only consist of a single amyloid-forming protein.[4,5] These deposits contain a range of different components, including other proteins, lipids, carbohydrates, and metal ions,[5] and all plaques do not contain exactly the same constituents.[6] A variety of different proteins have been found to be associated with senile plaques derived from brain autopsy of AD patients using, e.g., immunohistochemistry,[7−10] laser microdissection proteomics approaches[6,11,12] or spatially targeted optical microproteomics.[13] These studies have provided valuable knowledge about the AD pathology, but they are not able to distinguish between components that are integral parts of the plaques and those that are more loosely associated with the deposits or provide insights in the dynamics of the plaque's composition during build-up.

In a previous study, we reported that stabilized prefibrillar Aβ aggregates (protofibrils) are decorated with a range of human proteins when introduced in serum or cerebrospinal fluid (CSF).[14] Our findings emphasize that the pathological processes related to Aβ may not be fully understood from studies of experimental systems lacking the critical protein binding partners. This is in line with the pioneering work from Olzscha et al. which showed that a range of essential proteins are sequestered by artificial amyloid aggregates when expressed in a human cell model.[15] More recently, it has also been reported that amyloid fibrils of various origin attract "coronas" of binding proteins when introduced into a biological environment.[16−18] The role of protein coronas for the biological response is established for synthetic nanoparticles,[19] and it is now becoming evident that this phenomenon is also highly relevant to understand the biological activities of biomolecular nanoparticles, such as amyloid structures or virus particles.[20] From a more fundamental perspective, it can

Received: February 26, 2020
Accepted: April 21, 2020
Published: April 22, 2020

be noted that *any pathogenic process initiated by an amyloid aggregate must involve interactions between the aggregate and other (bio)molecules.* Hence, a detailed understanding of how the multiprotein aggregates that eventually develop into senile plaques are formed is crucial in order to achieve a molecular description of the pathological mechanisms.

Here, we present a bottom-up approach to isolate, identify, and quantitatively evaluate the components of the multiprotein aggregates that are formed around amyloid fibrils of Aβ(1−40) and Aβ(1−42), respectively, when introduced in human CSF (Figure 1) These are the two main variants of Aβ, with Aβ(1−42) being the more aggregation prone peptide.[2] CSF is used as model environment for the formation of senile plaques. Although this is not exactly the same environment as the brain parenchyma, CSF communicates freely with the brain interstitial fluid, which is the matrix in which the plaques are formed,[21] and Aβ levels in CSF have been shown to reflect brain amyloid load.[22] Clearly, the time frames of the study are also different than the cumulative buildup of plaques in Alzheimer patients, suggesting that the results primarily describe the composition of particles that may be early seeds for senile plaques. To explore if the disease progression affected the composition of the multiprotein aggregates, we compare CSF samples from AD patients and controls.

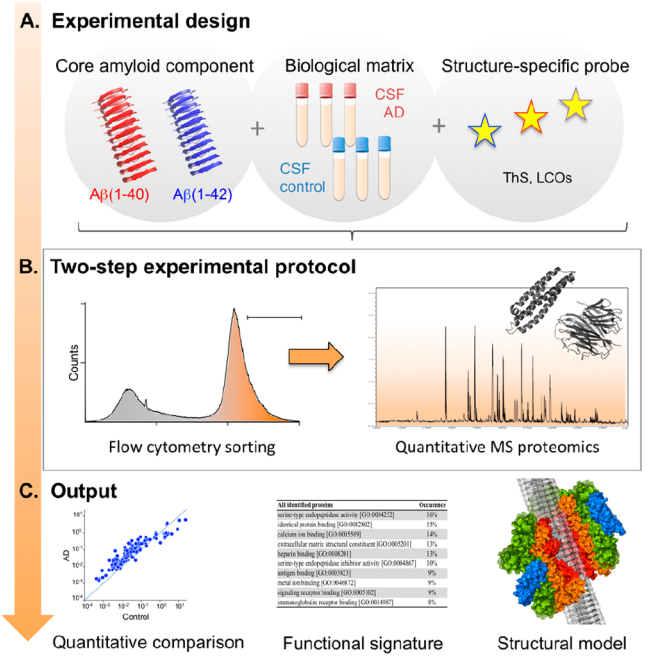

Figure 1. Schematic overview of the presented approach. (A) Experiments are designed by selecting different combinations of amyloid core component (i.e., fibrils from different peptides or with specific morphologies), biological matrix, and structure specific amyloid probes. (B) Selected components are mixed and multiprotein aggregates are isolated by flow cytometry. The components of these aggregates are then identified and quantified using MS. (C) We demonstrate how the results can be used for quantitative comparison of the components selected in the experimental design, provide functional signatures of the assembled complexes, and provide the basis for a building a structural model of the multiprotein aggregates.

The employed method is based on detection and sorting of the aggregates by flow cytometry (FC).[23,24] A similar approach was recently used to identify the protein components of "plaque particles" formed by spiking human serum with soluble Aβ, α-synuclein, tau, or cholesterol aggregates.[25] We have validated and further developed the methodology, which allows us to carry out a *quantitative* analysis of the compositions of the isolated multiprotein aggregates and propose a preliminary structural model.

RESULTS AND DISCUSSION

Preparation of Aβ Amyloid Aggregates. Recombinantly produced Aβ(1−40) and Aβ(1−42) were separately incubated at 37 °C for 48 h to produce fibrillar amyloid aggregates. Using recombinant peptides excluded the risk of contamination by other proteins that is associated with *in vivo*-derived Aβ samples. We chose to apply the same incubation conditions and incubation times, which we can easily control, for the two peptide variants rather than attempting to compare specific fibrillar morphologies, which are difficult to assess in a quantitative manner. After 48 h, fibrillation reached completion for both peptide variants,[26,27] and the presence of amyloid fibrils was confirmed by enhanced thioflavin T (ThT) fluorescence, circular dichroism (CD) spectra indicative of β-sheet structure, and the observation of fibrillar structures by atomic force microscopy (AFM) (SI Figure S1).

FC Detection of Aβ Aggregates in Biological Samples. Method development and validation were carried out using human serum. We first verified that Aβ amyloid aggregates bound to thioflavin S (ThS) can be detected by FC as previously reported by Madasamy et al.[25] The presence of particles is confirmed by the scattering plots (Figure 2A) and by a much higher particle count rate for samples containing Aβ compared to buffer-only samples (data not shown). Moreover, the Aβ-containing samples exhibited a distinct shift in fluorescence intensity compared to samples with ThS in serum (Figure 2), showing that the aggregates can be identified even in the complex background of a biological sample. We then used the described approach to isolate multiprotein aggregates for MS identification of binding proteins in human serum. In total, 126 and 125 binding proteins were found in samples spiked with Aβ(1−40) and Aβ(1−42) fibrils, respectively (SI Table S1).

FC and Pull-Down Experiments Are Complementary Methods. As a comparison we also carried out pull-down experiments using the same methodology as previously used for Aβ(1−42) protofibrils[14] and amyloid fibrils.[28] In these samples, 122 and 107 proteins were identified for Aβ(1−40) and Aβ(1−42), respectively (SI Table S1). Notably, the overlap between the proteins identified with FC sorting and the pull-down isolation is only about one-third (Figure 3C,D), indicating that the two methods provide complementary results. We also observed that with the FC method, 76% (i.e., 108 proteins) of the total number of identified proteins were found in both Aβ(1−40) and Aβ(1−42) samples, while the corresponding number for the pull-down approach is 25%. Out of these 25% (i.e., 44 proteins), 84% (37 proteins) are also found in the control experiments with glycine-coated beads (Figure 3A), suggesting that nonspecific binding affects the results for the pull-down approach, which makes quantitative analysis difficult. The control experiment for FC would be to isolate particles from a serum sample *without* added Aβ using the same sorting gates. It is evident from Figure 2B that essentially no such particles are detected.

Moreover, to validate the reproducibility of the methods we repeated the experiment three times with the same serum sample in separate analyses (referred to as the second batch in

https://dx.doi.org/10.1021/acschemneuro.0c00110
ACS Chem. Neurosci. XXXX, XXX, XXX−XXX

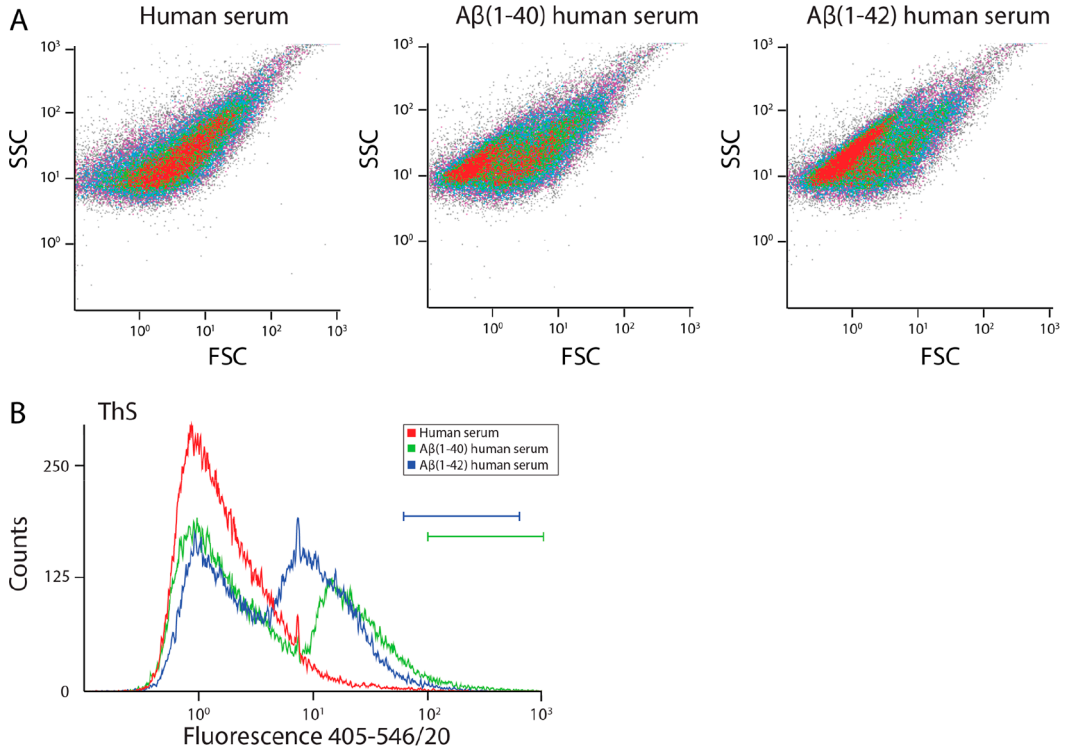

Figure 2. FC detection of Aβ aggregates in human serum. (A) Density plots from FC analysis of human serum only (left) and serum with added Aβ aggregates. Forward scatter intensity (FSC) is on the *x*-axis and side scatter intensity (SSC) on the *y*-axis. (B) Overlay of ThS fluorescence intensity histograms from FC analysis of samples with ThS (same runs as in panel A). The blue and green horizontal lines indicate the sorting gates used to isolate samples for MS analysis.

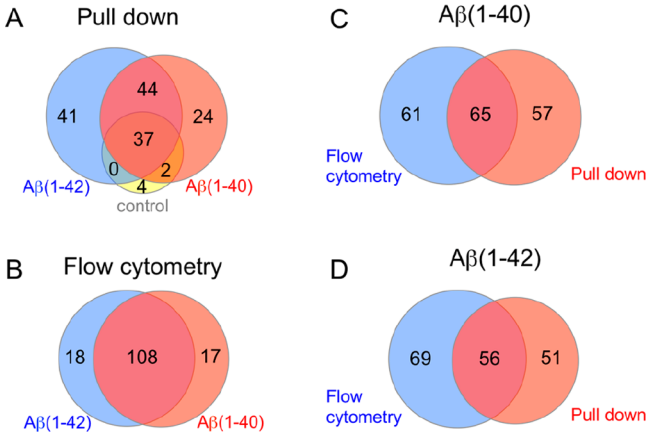

Figure 3. Comparison between pull-down and FC isolation of multiprotein aggregates. (A, B) Venn diagrams showing the number of proteins identified with the pull-down method for Aβ(1−40), Aβ(1−42), and glycine (control) coated magnetic beads, respectively (A), and the number of proteins identified with the FC sorting of Aβ(1−40) and Aβ(1−42) spiked samples, respectively (B). (C, D) Comparisons of the proteins identified in association with Aβ(1−40) (C) and Aβ(1−42) (D) with the two methods. Among the proteins that were identified by both methods, 30 and 32 proteins were also found in the pull-down control for Aβ(1−40) (C) and Aβ(1−42) (D), respectively.

the Methods section). With the FC method, 65% of the identified proteins were found in all three samples, while 20% were only found in one sample. For the pull-down approach, 37% were found in all three samples and 34% were only found in one sample. This indicates that the reproducibility of the FC method is higher than for the pull-down method.

Sensitivity Is Improved with LCO Probes. The experiments carried out so far demonstrated that ThS can detect amyloid structures. However, the use of newly developed amyloid probes could potentially improve both the sensitivity and the specificity of the method. Luminescent conjugated oligothiophenes (LCOs) is a group of compounds that have emerged as excellent probes of amyloid structures with the ability to distinguish between different classes of aggregates.[29] We examined three different LCOs in the FC setup: p-FTAA, which is a general amyloid ligand with the ability to detect most types of aggregates but with a higher sensitivity than ThT and ThS;[30] q-FTAA-CN, with a higher affinity for human brain-derived aggregates compared to synthetic fibrils;[31] and bTVBT2, which selectively recognizes tau aggregates in brain tissue.[32] From the results with serum samples spiked with Aβ(1−40) or Aβ(1−42) fibrils, we find that both p-FTAA and q-FTAA-CN provide improved separation between the amyloid aggregates and the serum background in the fluorescence distribution profiles compared to ThS (Figure 4). bTVBT2, on the other hand, shows a trend in the opposite direction, which is in line with the assumption that the multiprotein aggregates are formed around Aβ and not tau. Based on these results, we decided to use p-FTAA as probe for the experiments with human CSF samples.

Quantitative MS of CSF Samples. The formation of multiprotein aggregates was explored in human CSF samples from AD patients and non-AD controls (seven of each, SI Table S2) spiked with either Aβ(1−40) or Aβ(1−42) fibrils. The developed FC protocol was employed to isolate multiprotein aggregates for MS analysis from a total of 28 samples. Representative fluorescence distribution profiles are shown in SI Figure S2. Quantitative data were obtained

https://dx.doi.org/10.1021/acschemneuro.0c00110
ACS Chem. Neurosci. XXXX, XXX, XXX−XXX

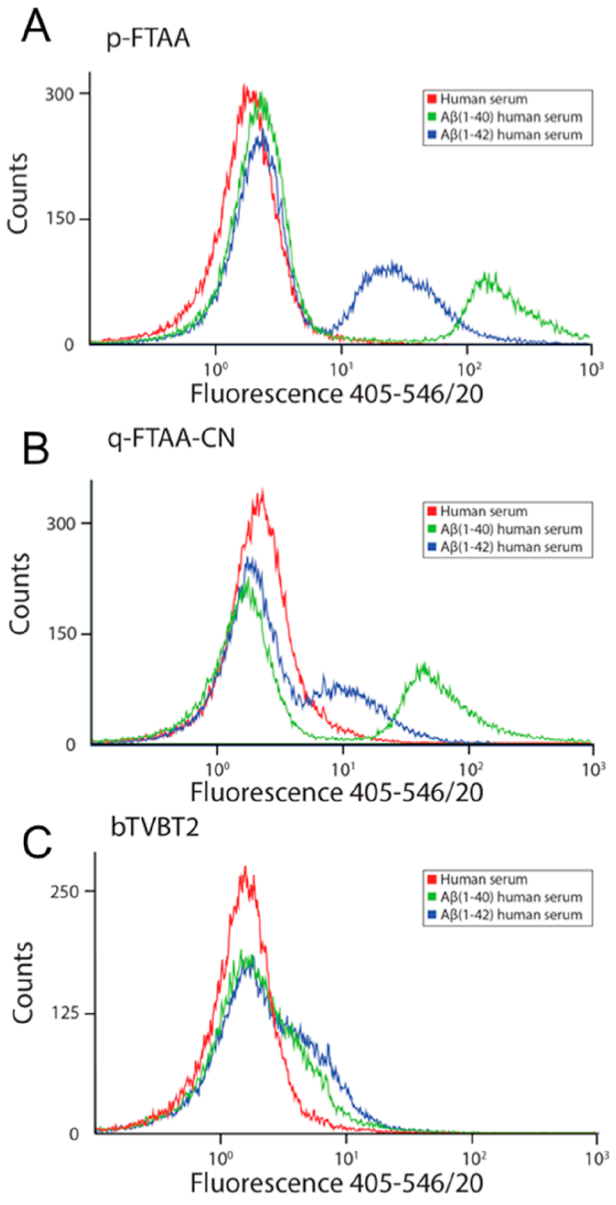

Figure 4. Overlay of LCO fluorescence intensity histograms from flow cytometry analysis of human serum only and serum with added Aβ aggregates. (A) p-FTAA probe. (B) q-FTAA-CN probe. (C) bTVBT2 probe.

through tandem mass tag (TMT) labeling, and the abundance values were normalized to the detected amount of Aβ in each sample. In total, 128 unique proteins, including Aβ, were detected and quantified (Table 1). The majority of the proteins (at least 82%) have previously been identified in senile plaques using microdissection techniques.[6,12] This supports our hypothesis that the presented results provide information about the assembly of senile plaques. In comparison with previous pull-down studies, we note that 58% of the identified proteins in our study overlap with the proteins reported to bind to Aβ(1−42) fibrils,[28] while 35% were also found to bind to prefibrillar aggregates modeled by Aβ(1−42)cc protofibrils.[14] The list (Table 1) contains several known amyloid precursor proteins,[33] e.g., transthyretin, β2-microglobulin, gelsolin, and apolipoproteins, which is in agreement with a previous study of the interactomes of selected amyloid fibrils.[16] There are also proteins that have been suggested as CSF biomarkers for AD,[34,35] e.g., chitinase-3-like protein 1, osteopontin, cystatin C, hemopexin, and zinc α-2 glycoprotein. Apolipoprotein E (apoE) and clusterin (apoJ), that are recognized genetic risk factors of AD[2], are both among the most abundant proteins (Figure 5 and Table 1).

The abundances of the proteins in CSF samples from AD patients and controls, respectively, are compared in Figure 5. Statistical analysis revealed one protein that is significantly enriched in the AD samples with Aβ(1−40) added (pyruvate kinase, $p = 8.8 \times 10^{-5}$) and two proteins that are significantly enriched in the AD samples with Aβ(1−42) added (alpha-2-HS-glycoprotein with $p = 0.030$ and prothrombin with $p = 0.024$). Increase in pyruvate kinase activity has been observed in the frontal and temporal cortex of AD brains[36] and the rabbit version of the enzyme inhibits the aggregation of Aβ(1−40).[37] Plasma levels of alpha-2-HS-glycoprotein has been found to be lower in AD patients than controls, potentially suggesting that the protein is sequestered in amyloid inclusions.[38] Prothrombin and its final product, thrombin, seems to be central in neurodegenerative processes associated with brain injury or disease.[39] A dysfunctional blood-brain barrier leads to (pro)thrombin entering the CNS and reaches high levels,[39] which might be related to the enrichment in AD samples. Prothrombin is also involved in tau proteolysis,[40] a process that is reduced for phosphorylated tau.

Functional Analysis of the Binding Proteins. Comparison of the abundances with selected properties of the proteins (such as size, charge, predicted solubility, or propensity to form amyloid) displayed no obvious correlations (SI Figure S3). Hence, we conclude that the binding of the identified proteins is not only a reflection of their physicochemical properties. This is in line with the results for the corona of IAPP amyloid fibrils.[18] Instead, we analyzed the list of identified proteins in terms of gene ontology (GO) annotations to explore the functional characteristics of the proteins bound to the Aβ amyloid aggregates. The most frequently occurring molecular function among all 127 binding proteins is serine-type endopeptidase activity (18%) followed by identical protein binding (15%) and calcium ion binding (14%) (SI Table S4). If we focus only on the 10% of the proteins with the highest average abundances in each sample type (SI Table S4), we find that identical protein binding is the most common function (39−46%) followed by amyloid-β binding (18%). The finding that several of the high abundance proteins are known Aβ-binding proteins provide some validation of the results. The results also indicate that proteins with an intrinsic ability to form homomultimeric structures might be more prone to bind to amyloid aggregates than what other proteins would be. The list of enriched functions among the top 10% binders also contains functionality related to lipid/cholesterol binding, which is in line with the fact that these molecules are often found in senile plaques.[5] For GO biological processes, the most frequent annotation among all the identified proteins is cellular protein metabolic process (21%), which is also the most frequent in the top 10% abundant proteins (46−62%) (SI Table S3). Hence, there is a direct link between the sequestering of proteins to the amyloid structures and changes in protein metabolism. The majority of the most frequently occurring processes are related to protein processing (e.g., cellular protein metabolic process or post-translational protein modification), defense mechanisms (e.g., immune response or complement activation), or vesicle transport (e.g., platelet- or neutrophil degranulation) (SI Table S3). GO cellular

https://dx.doi.org/10.1021/acschemneuro.0c00110
ACS Chem. Neurosci. XXXX, XXX, XXX−XXX

Table 1. Proteins Identified by MS in CSF[a]

Protein	Uniprot	Aβ(1-42) Control	Aβ(1-40) Control	Aβ(1-42) AD	Aβ(1-40) AD	Proto-fibrils *	Fibrils **	Senile plaques	Amyloid formation
Adipocyte enhancer-binding protein 1	Q8IUX7								
Afamin	P43652								
Alpha-1-acid glycoprotein 1	P02763								
Alpha-1-acid glycoprotein 2	P19652								
Alpha-1-antichymotrypsin	P01011								
Alpha-1-antitrypsin	A0A024R6I7								
Alpha-1B-glycoprotein	P04217								
Alpha-2-HS-glycoprotein	C9JV77								
Alpha-2-macroglobulin	P01023								
Amyloid-beta A4 protein	*P05067*								
Amyloid-like protein 1	P51693								
Angiotensinogen	P01019								
Antithrombin-III	P01008								
Apolipoprotein A-I	P02647								
Apolipoprotein A-II	V9GYM3								
Apolipoprotein A-IV	P06727								
Apolipoprotein C-III	B0YIW2								
Apolipoprotein D (Fragment)	C9JF17								
Apolipoprotein E	P02649								
Arginase-1	P05089								
Basement membrane-specific heparan sulfate proteoglycan core protein	P98160								
Beta-1,3-N-acetylglucosaminyltransferase lunatic fringe	Q8NES3								
Beta-1,4-glucuronyltransferase 1	O43505								
Beta-2-glycoprotein 1	P02749								
Beta-2-microglobulin	P61769								
Beta-Ala-His dipeptidase	Q96KN2								
Calsyntenin-1	O94985								
Cartilage acidic protein 1	Q9NQ79								
Ceruloplasmin	P00450								
Chitinase-3-like protein 1	P36222								
Cholecystokinin	P06307								
Clusterin	P10909								
Coagulation factor V	A0A0A0MRJ7								
Cofilin-1	P23528								
Collagen alpha-1(I) chain	P02452								
Collagen alpha-1(XVIII) chain	P39060								
Collagen alpha-2(I) chain	P08123								
Complement C1q subcomponent subunit B	P02746								
Complement C1q subcomponent subunit C	P02747								
Complement C1r subcomponent	B4DPQ0								
Complement C1s subcomponent	P09871								
Complement C3	P01024								
Complement C4-A / B	P0C0L4/5								
Complement factor B	P00751								
Complement factor H	P08603								
Corneodesmosin	Q15517								
Cystatin-C	P01034								
Decorin	P07585								
Dermcidin	P81605								
Desmocollin-1	Q08554								
Desmoplakin	P15924								
Dickkopf-related protein 3	F6SYF8								
Ectonucleotide pyrophosphatase/phosphodiesterase family member 2	Q13822								
Elastin	P15502								
Endoplasmin	P14625								
Extracellular matrix protein 2	O94769								
Extracellular superoxide dismutase [Cu-Zn]	P08294								
Fibrinogen alpha chain	P02671								
Fibrinogen beta chain	P02675								
Fibrinogen gamma chain	C9JC84								
Fibronectin	P02751								
Fibulin-7	Q53RD9								
Galectin-3-binding protein	Q08380								
Gelsolin	P06396								

Low High

https://dx.doi.org/10.1021/acschemneuro.0c00110
ACS Chem. Neurosci. XXXX, XXX, XXX−XXX

Table 1. continued

Protein	Uniprot	Aβ(1-42) Control	Aβ(1-40) Control	Aβ(1-42) AD	Aβ(1-40) AD	Proto-fibrils *	Fibrils **	Senile plaques	Amyloid formation
Growth arrest-specific protein 6	Q14393								
Haptoglobin	H0Y300								
Haptoglobin-related protein	P00739								
Hemoglobin subunit alpha	P69905								
Hemoglobin subunit beta	P68871								
Hemopexin	P02790								
Heparin cofactor 2	P05546								
Histidine protein methyltransferase 1 homolog	O95568								
Histidine-rich glycoprotein	P04196								
Ig heavy constant alpha 1	P01876								
Ig heavy constant alpha 2	P01877								
Ig heavy constant gamma 1	P01857								
Ig heavy constant gamma 2	P01859								
Ig heavy constant gamma 4	P01861								
Ig heavy variable 6-1	A0A0B4J1U7								
Ig kappa constant	P01834								
Ig kappa variable 3-20 / 3D-20	P01619								
Ig lambda constant 1 / Ig lambda-like polypeptide 5	P0CG04								
Ig lambda constant 2 / 3	P0DOY2/3								
Ig lambda constant 6 / 7	P0CF74 / A0M8Q6								
Ig lambda variable 1-47	P01700								
Inter-alpha-trypsin inhibitor heavy chain H1	P19827								
Inter-alpha-trypsin inhibitor heavy chain H4	Q14624								
Kallikrein-6	Q92876								
Kininogen-1	P01042								
L-lactate dehydrogenase A chain	P00338								
Latent-transforming growth factor beta-binding protein 4	Q8N2S1								
Mannosyl-oligosaccharide 1,2-alpha-mannosidase IA	P33908								
Microfibril-associated glycoprotein 4	K7ES70								
Mimecan	P20774								
Monocyte differentiation antigen CD14	P08571								
Neural cell adhesion molecule 1	A0A087WV75								
Neurosecretory protein VGF	O15240								
Olfactomedin-like protein 3	Q9NRN5								
Osteomodulin	Q99983								
Osteopontin	P10451								
Phosphoglycerate kinase 1	P00558								
Phospholipid transfer protein	P55058								
Pigment epithelium-derived factor	P36955								
Plasma protease C1 inhibitor	E9PGN7								
Procollagen C-endopeptidase enhancer 1	Q15113								
Prolargin	P51888								
ProSAAS	Q9UHG2								
Prosaposin	C9JIZ6								
Prostaglandin-H2 D-isomerase	P41222								
Proteoglycan 4	Q92954								
Prothrombin	P00734								
Prothymosin alpha	P06454								
Pyruvate kinase (Fragment)	H3BTN5								
Secreted frizzled-related protein 3	Q92765								
Secretogranin-1	P05060								
Selenoprotein P	P49908								
Serotransferrin	P02787								
SPARC-like protein 1	Q14515								
Spondin-1	Q9HCB6								
Sushi repeat-containing protein SRPX	P78539								
Testican-1	Q08629								
Thioredoxin	P10599								
Transthyretin	P02766								
Uncharacterized protein	E7ETN3								
Vitamin D-binding protein	D6RF35								
Vitamin K-dependent protein S	P07225								
Vitronectin	P04004								
Zinc-alpha-2-glycoprotein	P25311								

Low *High*

[a]Abundances (normalized) indicated by the color, from light red (low) to dark red (high). The binding to Aβ protofibrils and fibrils in previous (pull-down) studies are also shown with color-coding indicating in how many samples the proteins were found. In addition, the appearance in senile plaques (*ex vivo* samples) and the ability to form amyloid are indicated. *Ref 14. **Ref 28.

components is, as expected, strongly associated with extracellular space as CSF was used as biological sample (SI Table S5).

GO was also explored for the 10% most enriched proteins in either AD CSF or control CSF (SI Tables S6−S8). Interestingly, these lists highlight a different set of functional characteristics, except for the GO cellular components, which are essentially the same. For the GO biological process, the most enriched proteins lack the most common annotations found for the high abundance proteins, including cellular protein metabolic process, neutrophil degranulation, and all annotations and complement-related processes. Instead, negative regulation of blood coagulation and positive regulation of neurofibrillary tangle assembly, which are both highly relevant for AD pathology, are found among the top annotations. One should note that it is not the processes *per se* that are enriched but rather various proteins related to the processes. Hence, it is not strange that these annotations

https://dx.doi.org/10.1021/acschemneuro.0c00110
ACS Chem. Neurosci. XXXX, XXX, XXX−XXX

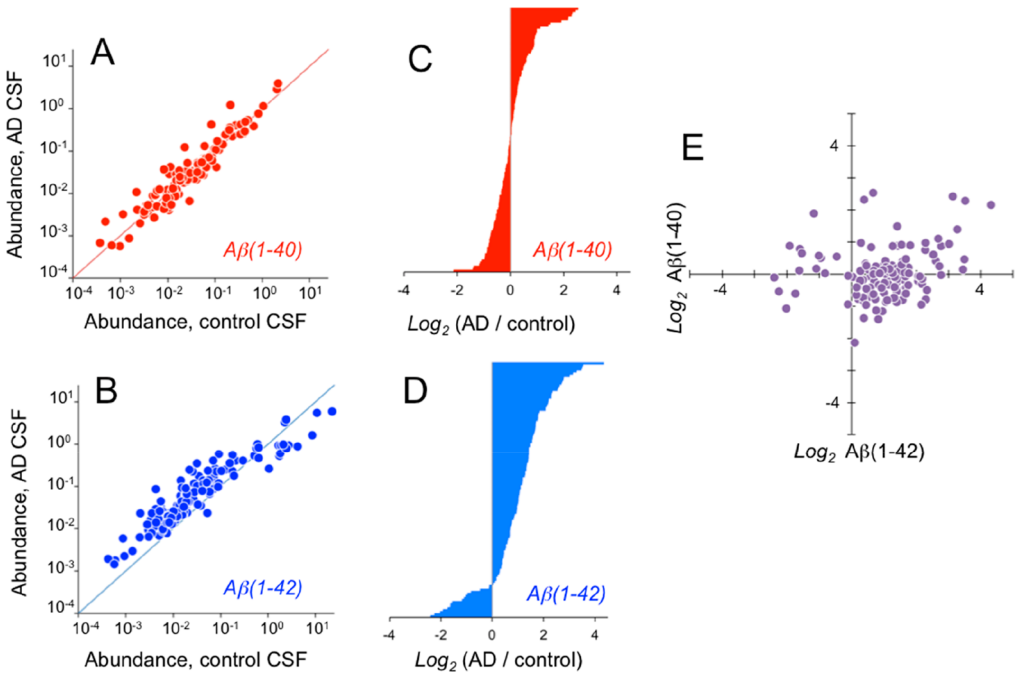

Figure 5. (A,B) Comparison of mean abundances in AD and control CSF samples, respectively, with the addition of Aβ(1−40) fibrils (A) and Aβ(1−42) fibrils (B). The diagonal lines are shown to guide the eye. (C,D) Comparison of mean abundances in AD and control CSF samples, respectively, shown as the ratio between AD and control (on a $\log_2$ scale). The data is displayed from lowest to highest values for proteins found in samples with Aβ(1−40) fibrils (C) and Aβ(1−42) fibrils (D). (E) Comparison the $\log_2$ ratios for Aβ(1−40) and Aβ(1−42).

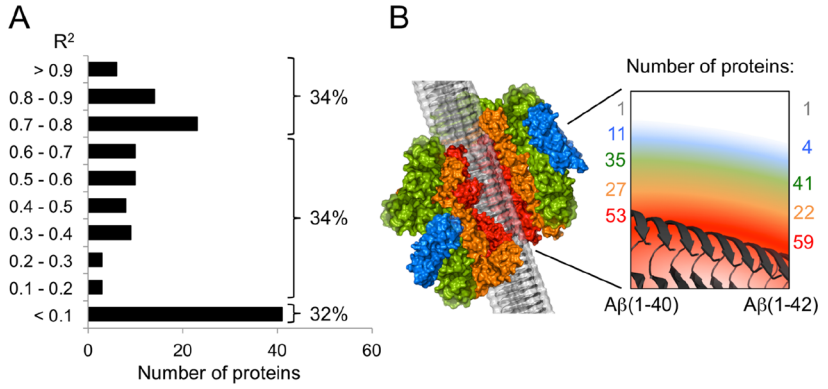

Figure 6. (A) Distribution of R^2-values for the correlations between the binding proteins and Aβ (in all analyzed CSF samples). (B) Model for the architecture of the multiprotein aggregates based on pairwise correlations between all proteins. The numbers indicate how many proteins that are found in each "layer". For Aβ(1−42), the number in blue includes both the fourth and fifth layers. All 14 samples for each Aβ variant were included in the analysis. The complete list of proteins in each layer is found SI Table S10.

appear among enriched proteins in both AD and control CSF. Notably, for GO molecular function, calcium ion binding appears as the most common annotation among the proteins enriched in the AD CSF samples (but not in control) for both Aβ(1−40) and Aβ(1−42). This may indeed be related to the fact that dysfunctional calcium homeostasis is a part of the AD pathology.[2]

Differences between Aβ(1−40) and Aβ(1−42). Figure 5A,B shows that there is a correlation between the abundances measured in AD and control CSF samples, as the points fall close to the diagonal. However, when considering the whole data sets, the patterns for Aβ(1−40) and Aβ(1−42) fibrils are different. For the Aβ(1−40) samples (Figure 5A), the points are evenly distributed around the diagonal line. For the Aβ(1−42) samples (Figure 5B), on the other hand, the majority of the identified proteins end up above the diagonal (meaning that they are enriched in AD CSF), while the proteins with the highest overall abundances instead seem to be enriched in the control samples. This feature is even more obvious when comparing the ratio between the abundances in AD and control samples (on a $\log_2$ scale, Figure 5C,D). In Aβ(1−40) samples, 49% of the proteins are enriched in the AD CSF samples while the corresponding number for Aβ(1−42) is 87%.

Although these findings are intriguing, the results should be interpreted with caution as significant differences were only found for a few proteins (see above). Moreover, the mechanisms that could give rise to the observed effect are not clear. The most obvious explanations can be rejected. If there were higher total protein concentrations in the AD samples, we would expect to see similar trends independent of the origin of the amyloid fibrils. The same line of arguments

https://dx.doi.org/10.1021/acschemneuro.0c00110
ACS Chem. Neurosci. XXXX, XXX, XXX−XXX

holds for explanations involving the pre-existence of amyloid aggregates in the AD CSF samples. If the difference instead were due to higher effective concentration of Aβ(1−42) fibrils compared to Aβ(1−40) fibrils (i.e., more available binding sites either through a larger amount of fibrils or a different morphology), we would expect to see more binding also for the control samples. Nevertheless, the results show that the two investigated Aβ variants gives distinct interactome responses.

We also investigated if there is a correlation between the Aβ(1−40) and Aβ(1−42) data in terms of in which type of CSF samples the proteins are enriched. The logarithmic abundance ratios for the two Aβ variants are compared in Figure 5E. The majority of proteins are found to be anticorrelated and found in the lower right quadrant, which is not surprising considering the graphs shown in Figure 5C,D. However, most of the points with the largest root-mean-square (RMS) are found to be enriched in AD CSF samples for both Aβ(1−40) and Aβ(1−42). These include, e.g., vitamin K-dependent protein, growth arrest-specific protein 6, and alpha-2-HS-glycoprotein. The full list of proteins in each quadrant is found in SI Table S9.

Architecture of Plaque Particles. Finally, we investigated if the generated data could provide information about how the early plaque particles are assembled. We hypothesize that for a protein that interacts directly with Aβ amyloid fibrils we should observe a correlation between the observed abundance of this protein and the abundance of Aβ in the investigated samples. The correlation might not be perfect because other proteins can affect the binding directly (e.g., as competing interaction partners) or indirectly (e.g., occupying the same binding sites on the amyloid structure). It will also depend on the initial level of the protein in the CSF samples. Nevertheless, we computed the coefficient of determination (R^2) for the correlation with Aβ abundance for all proteins, and we found that about one-third of the proteins have R^2 values above 0.7, while one-third have values below 0.1 (Figure 6A). Hence, it is unlikely that all identified proteins bind directly to Aβ. Considering the observed differences between amyloid fibrils of Aβ(1−40) and Aβ(1−42), we decided to analyze the data for each type amyloid aggregate separately. We computed the pairwise correlations for all the identified proteins and found that all proteins (but one) display at least one correlation with a R^2 value higher than 0.69 and 0.64 for Aβ(1−40) and Aβ(1−42), respectively. The only exception is prothymosin alpha, which is also the protein with the lowest overall abundance. Hence, the correlation analysis suggests that this might be a false positive. Using the values 0.69 and 0.64 for Aβ(1−40) and Aβ(1−42), respectively, as cut-offs, we constructed models for a layered architecture of the multiprotein aggregates (Figure 6B). In these models, proteins with high correlations with Aβ were assumed to interact directly with Aβ in the first layer. Then, all proteins with a high correlation to at least one protein in the first layer were defined to constitute the second layer and so on. The outcome of this analysis depends on the cutoff values, with an increasing number of proteins ending up outside the ten first layers if the cutoff is increased. With the employed cut off values, 53 and 59 proteins are found to bind directly (i.e., the first layer) to Aβ(1−40) and Aβ(1−42), respectively, and all proteins (except prothymosin alpha as mentioned) are included within 4 (Aβ1−40) or 5 (Aβ1−42) layers.

We can observe some differences when comparing the layer compositions for Aβ(1−40) and Aβ(1−42). Most of the differences reflect moving a protein from one layer to the adjacent layer (SI Table S10). This could be subtle effects of, e.g., the employed cutoff or the relative amounts of different binding partners present in the multiprotein complexes. However, a change from the direct binding layer to layers further out could indeed indicate processes that may be of pathological relevance. We note, for instance, that the complement-related proteins seem to have a higher degree of direct binding to Aβ(1−42) than for the Aβ(1−40) fibrils. Functional analysis (GO) of the layers is presented in SI Tables S11−S13. Although this data should be interpreted with caution (as it is still a crude model), we note that all proteins annotated with amyloid-β binding in GO molecular function are found in the first layer.

As a comparison, we also analyzed the protein interaction network by STRING[41] analysis. The generated network with color-coding from our multilayer models is shown in SI Figures S4 and S5. It is not obvious what to expect from this comparison, in particular, since the STRING interaction analysis does not distinguish native interactions from those involving the amyloid structure of Aβ. However, we note that Aβ (APP) appears at a very central position in the network and is surrounded by several red nodes (indicating direct binding to Aβ in our model). We also find that prothymosin alpha, the potential false positive mentioned above, ends up with no connections to the network. Moreover, the occurrence of highly connected networks suggest that it is plausible that many of the binding proteins could end up in the multiprotein aggregates due to secondary interactions (i.e., not direct binding to the amyloid fibrils). In the absence of experimental validation, the molecular details of the models should not be overinterpreted, but they propose that proteins may be incorporated in the deposits in different ways, which could affect their roles in the pathology.

CONCLUSIONS

In order to bring new light on the network of protein−protein interactions related to Aβ amyloid fibrils, we used and further developed an FC-based methodology to isolate multiprotein assemblies. We demonstrate its applicability for quantitative proteomics and show that the obtained results are complementary to the data from pull-down assays. The quantitative data allows us to analyze and compare the composition of the multiprotein aggregates based on different Aβ variants as well as the origin of CSF samples, and we observe distinct interactome responses for amyloid aggregates formed by Aβ(1−40) and Aβ(1−42), respectively. Functional analysis of the binding proteins identified several connections to known pathological processes of AD. Moreover, we demonstrate how the generated results could be used to build models of the architecture of multiprotein amyloid aggregates. Our data provide a first glimpse of this architecture, although the modeling approach needs further refinement and experimental validation. Taken together, we believe this work points out a new direction for the research aimed at understanding the assembly of protein inclusions involved in amyloid disorders. The developed method can easily be applied to a variety of experimental setups with different amyloid proteins, different biological samples, different fluorescence probes, and/or different incubation conditions and thereby lay the foundation for improved understanding of the biochemical processes

https://dx.doi.org/10.1021/acschemneuro.0c00110
ACS Chem. Neurosci. XXXX, XXX, XXX−XXX

leading to the formation of senile plaques as well as other protein deposits associated with neurodegeneration.

MATERIALS AND METHODS

Materials. Human serum (single normal healthy donor) was purchased from 3H Biomedical AB (Uppsala, Sweden). CSF samples were obtained from the Clinical Neurochemical Laboratory (Sahlgrenska University Hospital, Gothenburg, Sweden). CSF samples were from patients who sought medical advice because of cognitive impairment. Detailed information on the samples is shown in the Supporting Information Table S2. Lyophilized recombinant Aβ(1−40) and Aβ(1−42) peptides were purchased from rPeptide (Watkinsvill, GA, USA). LCOs were kindly provided by Peter Nilsson (Linköping University, Sweden).

Preparation of Amyloid Aggregates. Aβ peptide samples were prepared in sodium phosphate buffer pH 7.4 as described in ref 42. Amyloid fibrils were obtained by incubating the peptide samples with a concentration of 1 mg/mL at 37 °C with agitation (300 rpm) for 48 h. Fibril formation was confirmed by ThT fluorescence, AFM imaging, and far-UV CD spectroscopy. The amyloid fibril samples were stored at 4 °C during the complete set of experiments.

Pull-Down Assay. The amyloid fibrils were coupled to M-280 tosyl-activated Dynabeads (Invitrogen) as described in Rahman et al.[14] M-280 tosyl-activated Dynabeads coated with glycine were used as control.[14] For capturing proteins from human serum, 0.5 mg of beads coated with Aβ fibrils was added to 150 μL serum. The samples were incubated for 1 h at 37 °C and washed three times with PBS buffer (pH 7.4, with 0.1% Tween-20). The bound proteins were eluted in 12 μL SDS-PAGE Laemmli buffer (Bio Rad) supplemented with 50 mM 1,4-dithiothreitol (DTT from VWR) and heated to 70 °C for 10 min. The eluted samples were run on SDS-PAGE Mini-Protean 4−20% gradient gels from Bio-Rad. The gels were stained using AcquaStain (Lubio science, Zürich, Switzerland). Whole gel lanes, except for the regions containing Aβ (below 10 kDa), were extracted and analyzed by MS.

Flow Cytometry. Human serum was diluted 1:3 in PBS buffer pH 7.4, and 30 μg of Aβ fibrils was added to a final volume of 500 μL. The samples were incubated at 37 °C temperature for 30 min. ThS (Sigma) was added to a final concentration of 10 μM and samples were incubated at 37 °C for 10 min. For the sorting experiments with LCOs, samples were prepared as for ThS but with a final LCO concentration of 1.5 μM LCO (p-FTAA, q-FTAA-CN, or bTVBT2). For CSF samples, 20 μg of Aβ fibrils and p-FTAA corresponding to 1.5 μM final concentration were added to CSF to achieve a final volume of 500 μL. Isolation of multiprotein aggregates was performed at room temperature using a MoFlo Astrios EQ (Beckman Coulter).

Mass Spectrometry and Data Analysis. Protein concentrations were determined using a BCA kit from Pierce. The isolated samples were reduced, alkylated, and trypsin digested and thereafter analyzed by liquid chromatography and electrospray mass spectrometry. Quantitative data for the CSF samples were obtained using TMT-10plex labeling. Proteins were identified from the SwissProt database (HUMAN) using Mascot ver. 2.5.1 (MatrixScience Ltd., UK) database search engine. For qualitative analysis of serum samples, the list of hits was filtered to remove all entries with only a single peptide identified and all keratins (contaminations). Then, a threshold was set for each sample to achieve a false discovery rate (FDR) of less than 3%. Data with the TMT-labeled samples were analyzed on Proteome Discoverer ver. 2.2 (Thermo Scientific) using Mascot ver. 2.5.1 (MatrixScience Ltd., UK) database search engine. Keratins (contamination) were removed. The abundance was set to zero for proteins that were not detected in a specific sample, and the abundances were normalized using the abundance of Aβ (APP) in each sample.

Data Analysis. *p*-Values were calculated using the Student's *t*-test. For each protein, the differences in abundances of AD and control CSF samples were analyzed in terms of relative changes calculated as $\log_2$(Abundance in AD/Abundance in control). GO annotations for the identified proteins were extracted from the UniProt database (January 2019). The amino acid sequences from the Uniprot entries were used to predict the pI (from Proteome Discoverer ver. 2.2), charge at neutral pH (Expasy ProtParam), GRAVY (Expasy ProtParam), intrinsic solubility at pH 7 (CamSol[43]), and the propensity of amyloid aggregation (TANGO,[44,45] pH 7, 37 °C, ionic strength = 0.02 M, concentration = 1 M). Pairwise correlations between the protein abundances were computed using Matlab R2014b (MathWorks). STRING analysis[41] was performed using the web interface (string-db.org, ver. 11.0, 2019-08-27).

ASSOCIATED CONTENT

Supporting Information

The Supporting Information is available free of charge at https://pubs.acs.org/doi/10.1021/acschemneuro.0c00110.

Detailed materials and methods, biophysical characterization of Aβ amyloid fibrils, representative FC fluorescence intensity histograms of CSF samples, correlation analysis between protein abundance and selected physicochemical properties, STRING protein−protein interaction network analysis, correlations between APP abundance and average protein abundance and between APP abundance and the Aβ concentration in the CSF samples. Proteins identified in serum samples, information on analyzed CSF samples, GO functional analysis of all proteins, the most abundant proteins and of the proteins enriched in specific samples, positions of individual proteins in Figure 4e, proteins components in the layers of the structural model, GO functional analysis of the layers in the structural models. (PDF)

Comparison of FC and pull-down methods with serum—first batch (XLSX)

Comparison of FC and pull-down methods with serum—second batch (XLSX)

Identified proteins in CSF (XLSX)

Properties of the identified proteins (XLSX)

Pairwise correlations (XLSX)

AUTHOR INFORMATION

Corresponding Author

Christofer Lendel − *Department of Chemistry, KTH Royal Institute of Technology, Stockholm SE-100 44, Sweden;* orcid.org/0000-0001-9238-7246; Email: lendel@kth.se

Authors

Himanshu Chaudhary − *Department of Chemistry, KTH Royal Institute of Technology, Stockholm SE-100 44, Sweden*

Sebastian W. Meister − *Department of Protein Science, KTH Royal Institute of Technology, Stockholm SE-100 44, Sweden*

Henrik Zetterberg − *Department of Psychiatry and Neurochemistry, Institute of Neuroscience and Physiology, the Sahlgrenska Academy at the University of Gothenburg, Mölndal SE-413 90, Sweden; Clinical Neurochemistry Laboratory, Sahlgrenska University Hospital, Mölndal SE-413 90, Sweden; Department of Neurodegenerative Disease, UCL Institute of Neurology, London WC1N 3BG, United Kingdom; UK Dementia Research Institute at UCL, London WC1N 3BG, United Kingdom*

John Löfblom − *Department of Protein Science, KTH Royal Institute of Technology, Stockholm SE-100 44, Sweden;* orcid.org/0000-0001-9423-0541

Complete contact information is available at: https://pubs.acs.org/10.1021/acschemneuro.0c00110

https://dx.doi.org/10.1021/acschemneuro.0c00110
ACS Chem. Neurosci. XXXX, XXX, XXX−XXX

Author Contributions

H.C. and S.W.M. contributed equally. C.L. conceived of the idea and designed the study together with H.C., S.W.M., and J.L. H.C., S.W.M., and C.L. carried out experiments and analyzed data. H.Z. provided CSF samples and background information on these samples. All authors contributed to the writing of the manuscript.

Notes

The authors declare no competing financial interest.

■ ACKNOWLEDGMENTS

We are grateful to Peter Nilsson (Linköping University) for providing the LCO probes. Protein identification and quantification were carried out by the Proteomics Biomedicum core facility at Karolinska Institutet, Stockholm, Sweden (https://ki.se/en/mbb/proteomics-biomedicum). We thank Akos Vegvari for his helpful assistance. This work was supported by the Swedish Alzheimer Foundation (grants AF-544641, AF-640331, AF-733821 to C.L.) and the Swedish Research Council (grant 2016-03952 to C.L.). H.Z. is a Wallenberg Academy Fellow supported by grants from the Swedish Research Council (2018-02532), the European Research Council (681712), Swedish State Support for Clinical Research (ALFGBG-720931), and the UK Dementia Research Institute at UCL.

■ REFERENCES

(1) Chiti, F., and Dobson, C. M. (2006) Protein misfolding, functional amyloid, and human disease. *Annu. Rev. Biochem. 75*, 333−366.

(2) Querfurth, H. W., and LaFerla, F. M. (2010) Alzheimer's disease. *N. Engl. J. Med. 362*, 329−344.

(3) Cupino, T. L., and Zabel, M. K. (2014) Alzheimer's silent partner: cerebral amyloid angiopathy. *Transl. Stroke Res. 5*, 330−337.

(4) Armstrong, R. A., Lantos, P. L., and Cairns, N. J. (2008) What determines the molecular composition of abnormal protein aggregates in neurodegenerative disease? *Neuropathology 28*, 351−365.

(5) Stewart, K. L., and Radford, S. E. (2017) Amyloid plaques beyond A: a survey of the diverse modulators of amyloid aggregation. *Biophys. Rev. 9*, 405−419.

(6) Drummond, E., Nayak, S., Faustin, A., Pires, G., Hickman, R. A., Askenazi, M., Cohen, M., Haldiman, T., Kim, C., Han, X., Shao, Y., Safar, J. G., Ueberheide, B., and Wisniewski, T. (2017) Proteomic differences in amyloid plaques in rapidly progressive and sporadic Alzheimer's disease. *Acta Neuropathol. 133*, 933−954.

(7) Abraham, C. R., Selkoe, D. J., and Potter, H. (1988) Immunochemical identification of the serine protease inhibitor 1-antichymotrypsin in the brain amyloid deposits of Alzheimer's disease. *Cell 52*, 487−501.

(8) Kalaria, R. N., Golde, T., Kroon, S. N., and Perry, G. (1993) Serine-protease inhibitor antithrombin-III and its messenger-RNA in the pathogenesis of Alzheimers-disease. *Am. J. Pathol. 143*, 886−893.

(9) Nakamura, Y., Takeda, M., Suzuki, H., Hattori, H., Tada, K., Hariguchi, S., Hashimoto, S., and Nishimura, T. (1991) Abnormal distribution of cathepsins in the brain of patients with Alzheimers-disease. *Neurosci. Lett. 130*, 195−198.

(10) Navarro, A., del Valle, E., Astudillo, A., del Rey, C. G., and Tolivia, J. (2003) Immunohistochemical study of distribution of apolipoproteins E and D in human cerebral amyloid deposits. *Exp. Neurol. 184*, 697−704.

(11) Liao, L., Cheng, D., Wang, J., Duong, D. M., Losik, T. G., Gearing, M., Rees, H. D., Lah, J. J., Levey, A. I., and Peng, J. (2004) Proteomic characterization of postmortem amyloid plaques isolated by laser capture microdissection. *J. Biol. Chem. 279*, 37061−37068.

(12) Xiong, F., Ge, W., and Ma, C. (2019) Quantitative proteomics reveals distinct composition of amyloid plaques in Alzheimer's disease. *Alzheimer's Dementia 15*, 429−440.

(13) Hadley, K. C., Rakhit, R., Guo, H., Sun, Y., Jonkman, J. E., McLaurin, J., Hazrati, L. N., Emili, A., and Chakrabartty, A. (2015) Determining composition of micron-scale protein deposits in neurodegenerative disease by spatially targeted optical micro-proteomics. *eLife 4*, No. e09579.

(14) Rahman, M. M., Zetterberg, H., Lendel, C., and Härd, T. (2015) Binding of human proteins to amyloid-m protofibrils. *ACS Chem. Biol. 10*, 766−774.

(15) Olzscha, H., Schermann, S. M., Woerner, A. C., Pinkert, S., Hecht, M. H., Tartaglia, G. G., Vendruscolo, M., Hayer-Hartl, M., Hartl, F. U., and Vabulas, R. M. (2011) Amyloid-like aggregates sequester numerous metastable proteins with essential cellular functions. *Cell 144*, 67−78.

(16) Juhl, D. W., Risor, M. W., Scavenius, C., Rasmussen, C. B., Otzen, D., Nielsen, N. C., and Enghild, J. J. (2019) Conservation of the amyloid interactome across diverse fibrillar structures. *Sci. Rep. 9*, 3863.

(17) Nandakumar, A., Xing, Y., Aranha, R. R., Faridi, A., Kakinen, A., Javed, I., Koppel, K., Pilkington, E. H., Purcell, A. W., Davis, T. P., Faridi, P., Ding, F., and Ke, P. C. (2020) Human plasma protein corona of Ao amyloid and its impact on islet amyloid polypeptide cross-Seeding. *Biomacromolecules 21*, 988−998.

(18) Pilkington, E. H., Gustafsson, O. J. R., Xing, Y. T., Hernandez-Fernaud, J., Zampronio, C., Kakinen, A., Faridi, A., Ding, F., Wilson, P., Ke, P. C., and Davis, T. P. (2018) Profiling the serum protein corona of fibrillar human islet amyloid polypeptide. *ACS Nano 12*, 6066−6078.

(19) Lynch, I., Cedervall, T., Lundqvist, M., Cabaleiro-Lago, C., Linse, S., and Dawson, K. A. (2007) The nanoparticle-protein complex as a biological entity, a complex fluids and surface science challenge for the 21st century. *Adv. Colloid Interface Sci. 134−135*, 167−174.

(20) Ezzat, K., Pernemalm, M., Pålsson, S., Roberts, T. C., Järver, P., Dondalska, A., Bestas, B., Sobkowiak, M. J., Levanen, B., Sköld, M., Thompson, E. A., Saher, O., Kari, O. K., Lajunen, T., Ekström, E. S., Nilsson, C., Ishchenko, Y., Malm, T., Wood, M. J. A., Power, U. F., Masich, S., Linden, A., Sandberg, J. K., Lehtiö, J., Spetz, A. L., and El Andaloussi, S. (2019) The viral protein corona directs viral pathogenesis and amyloid aggregation. *Nat. Commun. 10*, 2331.

(21) Blennow, K., Hampel, H., Weiner, M., and Zetterberg, H. (2010) Cerebrospinal fluid and plasma biomarkers in Alzheimer disease. *Nat. Rev. Neurol. 6*, 131−144.

(22) Palmqvist, S., Zetterberg, H., Blennow, K., Vestberg, S., Andreasson, U., Brooks, D. J., Owenius, R., Hägerström, D., Wollmer, P., Minthon, L., and Hansson, O. (2014) Accuracy of brain amyloid detection in clinical practice using cerebrospinal fluid l-amyloid 42: a cross-validation study against amyloid positron emission tomography. *JAMA Neurol. 71*, 1282−1289.

(23) Trieschmann, L., Navarrete Santos, A., Kaschig, K., Torkler, S., Maas, E., Schatzl, H., and Bohm, G. (2005) Ultra-sensitive detection of prion protein fibrils by flow cytometry in blood from cattle affected with bovine spongiform encephalopathy. *BMC Biotechnol. 5*, 26.

(24) Yang, Y., Keene, D., Peskind, E. R., Galasko, D. R., Hu, S.-C., Cudaback, E., Wilson, A. M., Li, G., Yu, C.-E., Montine, K. S., Zhang, J., Baird, G. S., Hyman, B. T., and Montine, T. J. (2015) Cerebrospinal fluid particles in Alzheimer disease and Parkinson disease. *J. Neuropathol. Exp. Neurol. 74*, 672−687.

(25) Madasamy, S., Chaudhuri, V., Kong, R., Alderete, B., Adams, C. M., Knaak, T. D., Ruan, W., Wu, A. H., Bigos, M., and Amento, E. P. (2015) Plaque array method and proteomics-based identification of biomarkers from Alzheimer's disease serum. *Clin. Chim. Acta 441*, 79−85.

(26) Cohen, S. I., Linse, S., Luheshi, L. M., Hellstrand, E., White, D. A., Rajah, L., Otzen, D. E., Vendruscolo, M., Dobson, C. M., and Knowles, T. P. (2013) Proliferation of amyloid- 42 aggregates occurs

https://dx.doi.org/10.1021/acschemneuro.0c00110
ACS Chem. Neurosci. XXXX, XXX, XXX−XXX

through a secondary nucleation mechanism. *Proc. Natl. Acad. Sci. U. S. A. 110*, 9758−9763.
(27) Meisl, G., Yang, X., Hellstrand, E., Frohm, B., Kirkegaard, J. B., Cohen, S. I., Dobson, C. M., Linse, S., and Knowles, T. P. (2014) Differences in nucleation behavior underlie the contrasting aggregation kinetics of the A 40 and A442 peptides. *Proc. Natl. Acad. Sci. U. S. A. 111*, 9384−9389.
(28) Rahman, M. M., Westermark, G. T., Zetterberg, H., Härd, T., and Sandgren, M. (2018) Protofibrillar and fibrillar amyloid-m binding proteins in cerebrospinal fluid. *J. Alzheimer's Dis. 66*, 1053−1064.
(29) Klingstedt, T., and Nilsson, K. P. (2012) Luminescent conjugated poly- and oligo-thiophenes: optical ligands for spectral assignment of a plethora of protein aggregates. *Biochem. Soc. Trans. 40*, 704−710.
(30) Åslund, A., Sigurdson, C. J., Klingstedt, T., Grathwohl, S., Bolmont, T., Dickstein, D. L., Glimsdal, E., Prokop, S., Lindgren, M., Konradsson, P., Holtzman, D. M., Hof, P. R., Heppner, F. L., Gandy, S., Jucker, M., Aguzzi, A., Hammarström, P., and Nilsson, K. P. R. (2009) Novel pentameric thiophene derivatives for in vitro and in vivo optical imaging of a plethora of protein aggregates in cerebral amyloidoses. *ACS Chem. Biol. 4*, 673−684.
(31) Bäck, M., Appelqvist, H., LeVine, H., and Nilsson, K. P. R. (2016) Anionic oligothiophenes compete for binding of X-34 but not PIB to recombinant Ae amyloid fibrils and Alzheimer's disease brain-derived Ai. *Chem. - Eur. J. 22*, 18335−18338.
(32) Shirani, H., Appelqvist, H., Bäck, M., Klingstedt, T., Cairns, N. J., and Nilsson, K. P. R. (2017) Synthesis of thiophene-based optical ligands that selectively detect tau pathology in Alzheimer's disease. *Chem. - Eur. J. 23*, 17127−17135.
(33) Sipe, J. D., Benson, M. D., Buxbaum, J. N., Ikeda, S. I., Merlini, G., Saraiva, M. J., and Westermark, P. (2016) Amyloid fibril proteins and amyloidosis: chemical identification and clinical classification International Society of Amyloidosis 2016 Nomenclature Guidelines. *Amyloid 23*, 209−213.
(34) Paterson, R. W., Heywood, W. E., Heslegrave, A. J., Magdalinou, N. K., Andreasson, U., Sirka, E., Bliss, E., Slattery, C. F., Toombs, J., Svensson, J., Johansson, P., Fox, N. C., Zetterberg, H., Mills, K., and Schott, J. M. (2016) A targeted proteomic multiplex CSF assay identifies increased malate dehydrogenase and other neurodegenerative biomarkers in individuals with Alzheimer's disease pathology. *Transl. Psychiatry 6*, No. e952.
(35) Roher, A. E., Maarouf, C. L., Sue, L. I., Hu, Y., Wilson, J., and Beach, T. G. (2009) Proteomics-derived cerebrospinal fluid markers of autopsy-confirmed Alzheimer's disease. *Biomarkers 14*, 493−501.
(36) Bigl, M., Bruckner, M. K., Arendt, T., Bigl, V., and Eschrich, K. (1999) Activities of key glycolytic enzymes in the brains of patients with Alzheimer's disease. *J. Neural Transm. 106*, 499−511.
(37) Luo, J., Wärmlander, S. K., Gräslund, A., and Abrahams, J. P. (2014) Non-chaperone proteins can inhibit aggregation and cytotoxicity of Alzheimer amyloid peptide. *J. Biol. Chem. 289*, 27766−27775.
(38) Smith, E. R., Nilforooshan, R., Weaving, G., and Tabet, N. (2011) Plasma fetuin-A is associated with the severity of cognitive impairment in mild-to-moderate Alzheimer's disease. *J. Alzheimer's Dis. 24*, 327−333.
(39) Krenzlin, H., Lorenz, V., Danckwardt, S., Kempski, O., and Alessandri, B. (2016) The importance of thrombin in cerebral injury and disease. *Int. J. Mol. Sci. 17*, E84.
(40) Arai, T., Miklossy, J., Klegeris, A., Guo, J. P., and McGeer, P. L. (2006) Thrombin and prothrombin are expressed by neurons and glial cells and accumulate in neurofibrillary tangles in Alzheimer disease brain. *J. Neuropathol. Exp. Neurol. 65*, 19−25.
(41) Szklarczyk, D., Gable, A. L., Lyon, D., Junge, A., Wyder, S., Huerta-Cepas, J., Simonovic, M., Doncheva, N. T., Morris, J. H., Bork, P., Jensen, L. J., and Mering, C. (2019) STRING v11: protein-protein association networks with increased coverage, supporting functional discovery in genome-wide experimental datasets. *Nucleic Acids Res. 47*, D607−D613.
(42) Abelein, A., Bolognesi, B., Dobson, C. M., Gräslund, A., and Lendel, C. (2012) Hydrophobicity and conformational change as mechanistic determinants for nonspecific modulators of amyloid self-assembly. *Biochemistry 51*, 126−137.
(43) Sormanni, P., Aprile, F. A., and Vendruscolo, M. (2015) The CamSol method of rational design of protein mutants with enhanced solubility. *J. Mol. Biol. 427*, 478−490.
(44) Fernandez-Escamilla, A. M., Rousseau, F., Schymkowitz, J., and Serrano, L. (2004) Prediction of sequence-dependent and mutational effects on the aggregation of peptides and proteins. *Nat. Biotechnol. 22*, 1302−1306.
(45) Linding, R., Schymkowitz, J., Rousseau, F., Diella, F., and Serrano, L. (2004) A comparative study of the relationship between protein structure and -aggregation in globular and intrinsically disordered proteins. *J. Mol. Biol. 342*, 345−353.

https://dx.doi.org/10.1021/acschemneuro.0c00110
ACS Chem. Neurosci. XXXX, XXX, XXX−XXX